Japanese Journal of Applied Physics
Vol. 45, No. 4A, 2006, pp. 2606–2611

Luminescence and Energy Transfer Characteristics of Tb^{3+}- and Ce^{3+}-Codoped $BaBPO_5$ Phosphors

Chung-Hsin LU*, Shrikant Vasant GODBOLE and Mohammad QURESHI

Electronic and Electro-optical Ceramics Laboratory, Department of Chemical Engineering, National Taiwan University, Taipei, Taiwan, R.O.C.

(Received June 7, 2005; revised November 14, 2005; accepted December 20, 2005; published online April 7, 2006)

The luminescence properties of barium borate phosphate phosphors doped with trivalent terbium ions and the effects of codoping cerium and sodium ions on their emission characteristics were investigated. $BaBPO_5$:Tb^{3+} phosphors exhibit intense green emissions upon excitation at 230 nm. The emissions can be assigned to various $^5D_4 \rightarrow {}^7F_J$ ($J = 3$, 4, 5, and 6) transitions of Tb^{3+} ions. Excitation in the 200–230 nm range in $BaBPO_5$:Tb^{3+} is ascribed to spin-allowed transitions. The relatively weak excitation band at 268 nm is attributed to spin-forbidden transitions. The codoping of Ce^{3+} ions along with Tb^{3+} in $BaBPO_5$ results in Tb^{3+} emissions and the quenching of Ce^{3+} emissions. Energy transfer from Ce^{3+} ions to Tb^{3+} ions increases with an increase in Ce^{3+} content. The codoping of sodium ions in terbium and cerium ions-doped $BaBPO_5$ phosphors leads to luminescence enhancement. This enhancement is attributed to the reduction in non-radiative losses. These investigations reveal that the phosphors containing Tb^{3+}, Ce^{3+}, and Na^+ ions in the $BaBPO_5$ host have potential for applications as green phosphors for tricolor lamps. [DOI: 10.1143/JJAP.45.2606]

KEYWORDS: phosphors, $BaBPO_5$, luminescence properties, energy transfer

1. Introduction

The alkaline earth borophosphates $MBPO_5$ (M = Ca, Sr, Ba) belong to the stillwellite-type compounds. It has been found that the compounds $MBPO_5$ share an isostructure that contains the anionic units of BO_4 and PO_4 tetrahedra connected by common corners. The arrangements of BO_4 and PO_4 are loop-branched chains.[1)] The spectroscopic properties of rare-earth ions in different hosts in the vacuum UV (VUV) range have attracted considerable attention in recent years. The design of the phosphors for tricolor fluorescent lamps is of great research interest. In particular, terbium-ion-incorporated materials with a sharp green emission with a typical $^5D_4 \rightarrow {}^7F_J$ ($J = 3, 4, 5, 6$) transition of Tb^{3+} ions and a predominant $^5D_4 \rightarrow {}^7F_5$ transition peaking at around 545 nm are utilized as lamp phosphors, CRT phosphors and X-ray imaging phosphors. Because of the potential application of terbium-ion-doped phosphors in illumination devices, a number of hosts such as borates, oxysulphides, silicates, garnets and phosphates have been investigated.[2–9)] In particular, $LaPO_4$, Y_2SiO_5, $CeMgAl_{11}O_{19}$, and $GdMgB_5O_{10}$ are some of the well-established phosphor materials in the lamp industry. The efficient green emission from these phosphors upon excitation at 254 nm is based on energy transfer from Ce^{3+} ions to Tb^{3+} ions.[10–14)] The importance of the energy transfer process in these phosphors has resulted in investigations into prospective host materials for activation with individual terbium ions and codoping terbium ions along with cerium ions.

Luminescence studies on new host materials activated with terbium ions have been reported.[15–19)] These studies also include phosphor materials based on Ce^{3+}- and Tb^{3+}-codoped systems involving energy transfer.[20–22)] Few studies involving the luminescence properties of activator ions, such as Ce^{3+}, Eu^{2+}, and Sm^{2+}, in the host $MBPO_5$ (M = Ca, Sr, Ba) have been investigated.[23–29)] Recently, the synthesis and photoluminescence properties of Tb^{3+}-doped $CaBPO_5$[30,31)] and $BaBPO_5$[32)] have been studied. The structural and luminescence properties of these borophosphates suggest that these phosphors are potential hosts for rare-earth ion luminescence.

In this study, the luminescence properties of trivalent terbium ions along with co-activators, such as Ce^{3+} and Na^+, were investigated in a $BaBPO_5$ host. The effect of sodium was two fold, as it partially acted as the flux and mainly as the barrier for reducing non-radiative transitions to enhance the efficiency of phosphors. This study was also intended to understand the luminescence and energy transfer characteristics between the doped ions and the host matrix. These results obtained reveal that $BaBPO_5$:Tb^{3+}, Ce^{3+}, and Na^+ phosphors have an intense green luminescence with an intensity comparable to commercially known green lamp phosphors.

2. Experimental

$BaBPO_5$ phosphors were prepared using solid-state reactions at high temperatures. For the preparation of $Ba_{1-m}Tb_mBPO_5$, where $m = 0.005$, 0.01, 0.05, and 0.1, reagent-grade $BaCO_3$, Tb_4O_7, $(NH_4)_2HPO_4$, and H_3BO_3 were thoroughly mixed in stoichiometric quantities by grinding. Boric acid was added nearly 1 wt% excess owing to its loss during high-temperature synthesis. In addition to Tb^{3+} ions, Na^+ and Ce^{3+} ions were codoped in the host matrix to investigate the energy transfer processes and codoping effects. These phosphors were prepared by adding appropriate quantities of Na_2HPO_4 and CeO_2 to obtain $Ba_{1-x-y}Tb_xCe_yBPO_5$ and $Ba_{1-x-y-z}Tb_xCe_yNa_zPO_5$ ($x = 0.1$, $y = 0.0005–0.01$, and $z = 0.005–0.05$). The corresponding mixtures were initially heated at 400 °C for 2 h in an air atmosphere. The phosphors were subsequently prepared by heating at 900 °C for 4 h in air. To ensure tetravalent terbium and cerium ions the conversion of into the trivalent state, these samples were subjected to a reduction treatment at 900 °C for 4 h in a mixed gas atmosphere (95 vol% N_2 and 5 vol% H_2).

The crystal structures of the prepared powders were examined via X-ray diffraction (XRD) studies using an X-ray diffractometer (MAC M03 XHF). The XRD pattern

*To whom all correspondence should be addressed.
E-mail address: chlu@ccms.ntu.edu.tw

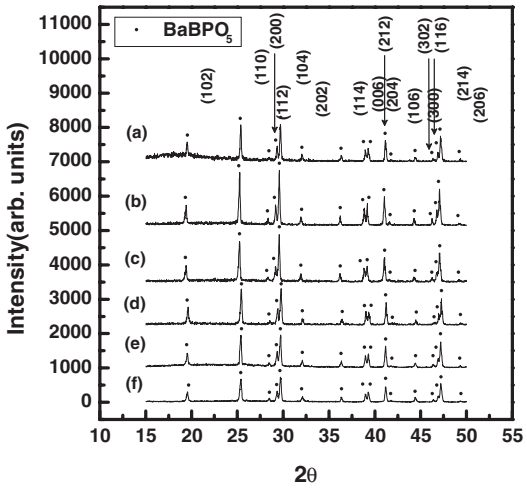

Fig. 1. XRD patterns for powders prepared by heating at 900 °C for 4 h in reducing atmosphere: (a) $Ba_{0.995}Tb_{0.005}BPO_5$, (b) $Ba_{0.99}Tb_{0.01}BPO_5$, (c) $Ba_{0.95}Tb_{0.05}BPO_5$, (d) $Ba_{0.9}Tb_{0.1}BPO_5$, (e) $Ba_{0.89}Tb_{0.1}Ce_{0.01}BPO_5$, and (f) $Ba_{0.84}Tb_{0.1}Ce_{0.01}Na_{0.05}BPO_5$.

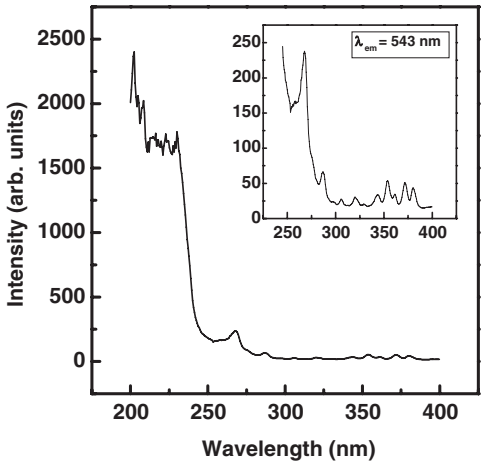

Fig. 2. Excitation spectra ($\lambda_{em} = 543$ nm) for 900 °C-heated $Ba_{0.9}Tb_{0.1}BPO_5$ in reducing atmosphere. Inset: excitation spectra in wavelength range of 245 to 500 nm.

analysis was performed to determine the chemical purity and phase homogeneity of the prepared powders. A field emission scanning electron microscope (SEM; Hitachi, S-800) was used to observe the microstructure of the prepared powders. Photoluminescence studies were conducted using a fluorescence spectrometer (Hitachi, F-4500). All the measurements were carried out, maintaining an excitation slit of 1 nm and emission slit of 2.5 nm with a power of 700 V using an Xe lamp (400 W).

3. Results and Discussion

3.1 Luminescence characteristics of terbium-ion-doped $BaBPO_5$ phosphors

The XRD patterns of samples prepared via a solid-state reaction are shown in Fig. 1. Figures 1(a)–1(d) illustrate the XRD patterns for $Ba_{0.995}Tb_{0.005}BPO_5$, $Ba_{0.99}Tb_{0.01}BPO_5$, $Ba_{0.95}Tb_{0.05}BPO_5$ and $Ba_{0.9}Tb_{0.1}BPO_5$ heated at 900 °C for 4 h in reducing atmosphere (95 vol % N_2 and 5 vol % H_2), respectively. These XRD patterns are similar to that reported for the compound barium borophosphate.[33] No secondary phases were observed in any of the prepared phosphors. These observations suggest that monophasic phosphors can be synthesized via heating at 900 °C with terbium ions replacing barium ions up to 10 at. %. The representative XRD patterns obtained for the samples with codopants are illustrated in Figs. 1(e) and 1(f) for the $Ba_{0.89}Tb_{0.1}Ce_{0.01}BPO_5$ and $Ba_{0.84}Tb_{0.1}Ce_{0.01}Na_{0.05}BPO_5$ samples. As illustrated in the figures, the XRD patterns obtained for these phosphors matched that reported for $BaBPO_5$. Since no additional XRD peaks are observed in these samples as a result of codoping terbium, cerium and sodium ions, it is evident that the powders obtained by the solid-state synthesis route are monophasic compounds.

Figure 2 illustrates the excitation spectra observed for a 543 nm emission in $Ba_{0.9}Tb_{0.1}BPO_5$. The inset shows the excitation spectra in the 250–400 nm wavelength range. A strong excitation (200–230 nm) along with a number of weak excitation peaks (250–380 nm) was observed for Tb^{3+} ions in the $BaBPO_5$ host. Among the weak excitation peaks illustrated in the inset, the excitation peak at 268 nm is relatively intense. The excitation peak at 380 nm is due to the $^7F_6 \rightarrow {}^5D_3$ transition. A number of weak excitation peaks in the 280–375 nm region is due to transitions between $^7F_6$ and the various excited states belonging to the f^8 electronic configuration of Tb^{3+} ions.

A strong excitation band due to spin-allowed ($4f^8 \rightarrow 4f^75d^1$) transition and a relatively weak band at a lower energy position due to spin-forbidden transition ($4f^8 \rightarrow 4f^75d^1$) have been reported for Tb^{3+} ions.[34–36] The strong excitation bands in the 200–230 nm region and the relatively weak band at 268 nm in $Ba_{0.9}Tb_{0.1}BPO_5$, as illustrated in Fig. 2, are probably due to the spin-allowed and spin-forbidden transitions of Tb^{3+} ions involving the $4f^8$ and $4f^75d$ electronic configurations in the ground and excited states, respectively. This confirms the report on $Ba_{0.97}Tb_{0.03}BPO_5$:Tb^{3+}.[32]

Figure 3(a) illustrates the emission spectra for $Ba_{0.9}Tb_{0.1}BPO_5$ in the 475–650 nm range obtained on 268 nm excitation. The emissions from Tb^{3+} ions occurring at 490, 543, 587, and 620 nm are due to the $^5D_4 \rightarrow {}^7F_6$, $^5D_4 \rightarrow {}^7F_5$,

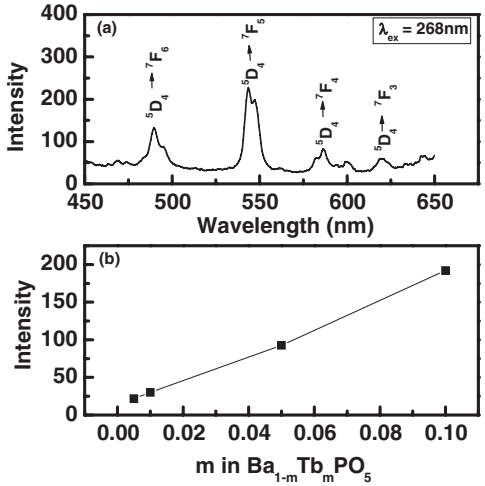

Fig. 3. (a) Emission spectra ($\lambda_{ex} = 268$ nm) of $Ba_{0.9}Tb_{0.1}BPO_5$ heated at 900 °C in reducing atmosphere. (b) Variation in emission intensity as a function of m in $Ba_{1-m}Tb_mBPO_5$ prepared by heating in reducing atmosphere at 900 °C ($\lambda_{ex} = 268$ nm and $\lambda_{em} = 543$ nm).

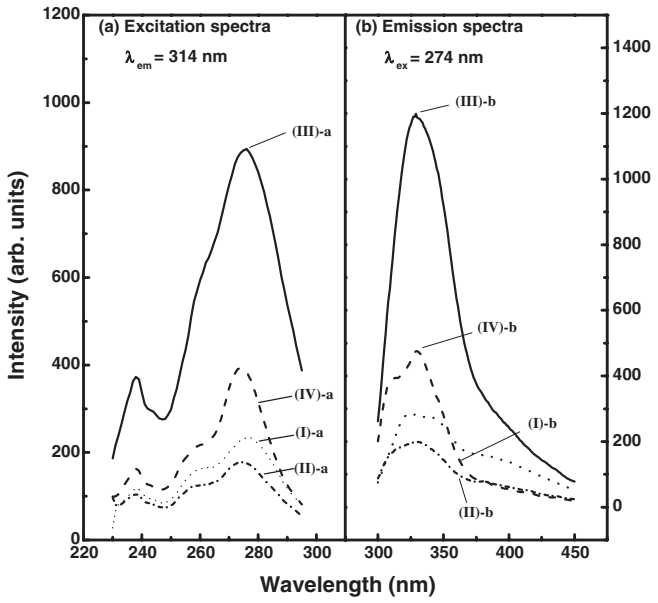

Fig. 4. Emission ($\lambda_{ex} = 274$ nm) and excitation spectra ($\lambda_{em} = 314$ nm) for phosphors prepared by heating at 900 °C for 4 h in reducing atmosphere: (I) $Ba_{0.99}Ce_{0.01}BPO_5$ (curves I-a and I-b), (II) $Ba_{0.89}Tb_{0.1}Ce_{0.01}BPO_5$ (curves II-a and II-b), (III) $Ba_{0.99}Ce_{0.01}Na_{0.05}BPO_5$ (curves III-a and III-b), and (IV) $Ba_{0.84}Tb_{0.1}Ce_{0.01}Na_{0.05}BPO_5$ (curves IV-a and IV-b). The symbols a and b indicate the excitation and emission spectra, respectively.

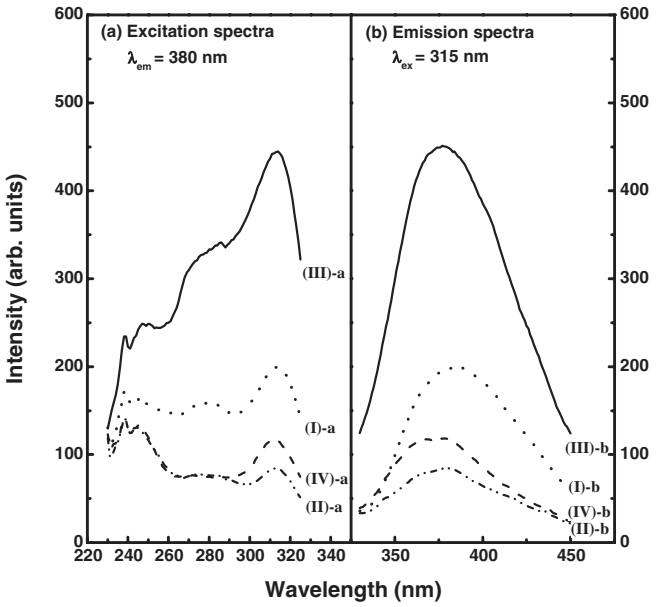

Fig. 5. Emission ($\lambda_{ex} = 315$ nm) and excitation spectra ($\lambda_{em} = 380$ nm) for phosphors prepared by heating at 900 °C for 4 h in reducing atmosphere: (I) $Ba_{0.99}Ce_{0.01}BPO_5$ (curves I-a and I-b), (II) $Ba_{0.89}Tb_{0.1}Ce_{0.01}BPO_5$ (curves II-a and II-b), (III) $Ba_{0.99}Ce_{0.01}Na_{0.05}BPO_5$ (curves III-a and III-b), and (IV) $Ba_{0.84}Tb_{0.1}Ce_{0.01}Na_{0.05}BPO_5$ (curves IV-a and IV-b). The symbols a and b indicate the excitation and emission spectra, respectively.

$^5D_4 \rightarrow {}^7F_4$, and $^5D_4 \rightarrow {}^7F_3$ transitions, respectively. Figure 3(b) illustrates the emission intensity at 543 nm for $Ba_{1-m}Tb_mBPO_5$ on 268 nm excitation. The peak intensity increases with the Tb^{3+} ion concentration in the $Ba_{1-m}Tb_mBPO_5$ samples. The results suggest that concentration quenching does not occur for the green emission from the terbium-ion-doped $BaBPO_5$ up to 10 at. % substitution.

3.2 Energy Transfer from Ce^{3+} ions to Tb^{3+} ions in $BaBPO_5$

Figure 4 illustrates the excitation ($\lambda_{em} = 314$ nm) and emission ($\lambda_{ex} = 275$ nm) spectra for Ce^{3+} ions in (I) $Ba_{0.99}Ce_{0.01}BPO_5$, (II) $Ba_{0.89}Tb_{0.1}Ce_{0.01}BPO_5$, (III) $Ba_{0.94}Ce_{0.01}Na_{0.05}BPO_5$, and (IV) $Ba_{0.84}Tb_{0.1}Ce_{0.01}Na_{0.05}BPO_5$ phosphors. It is observed that the excitation spectra of all samples show intense and broad excitation peaks at 275 and 237 nm, while the emission spectra of these samples reveal an emission peak at 320 nm. Figure 5 illustrates the excitation ($\lambda_{em} = 380$ nm) and emission ($\lambda_{ex} = 315$ nm) spectra for Ce^{3+} ions in (I) $Ba_{0.99}Ce_{0.01}BPO_5$, (II) $Ba_{0.89}Tb_{0.1}Ce_{0.01}BPO_5$, (III) $Ba_{0.94}Ce_{0.01}Na_{0.05}BPO_5$, and (IV) $Ba_{0.84}Tb_{0.1}Ce_{0.01}Na_{.05}BPO_5$ phosphors. The excitation spectra of these samples show a broad peak at 315 nm along with shoulder-like peaks at 274 and 237 nm. The emission spectra reveal a broad emission occurring at 380 nm.

The characteristic emission at 320 nm with excitation peaks at 237 and 275 nm, and the emission at 380 nm with excitation peaks at 315, 274, and 237 nm occur for the cerium-ion-doped $BaBPO_5$ samples. The incorporation of Ce^{3+} ions at the Ba^{2+} sites in the $BaBPO_5$ host requires the formation of charge compensatory vacancies to preserve the charge balance. Three Ba^{2+} ions can be replaced by two Ce^{3+} ions at barium sites, leaving one vacant Ba^{2+} site. This results in two different sites for Ce^{3+} ions in $BaBPO_5$, depending on whether such charge compensatory vacancies are associated with Ce^{3+} ions or not. In strontium borate and strontium halo borate, the emission at a short wavelength is ascribed to Ce^{3+} ions located at the Sr^{2+} sites without the involvement of an associated charge compensatory vacancy. The emission at a long wavelength is attributed to Ce^{3+} ions associated with the charge compensatory vacancy.[37,38] In view of these conditions, the emission of Ce^{3+} ions observed at 320 nm can be attributed to Ce^{3+} ions occupying Ba^{2+} sites without an associated charge compensatory vacancy (Site I). Conversely, the emission at 380 nm observed upon long wavelength excitation (315 nm) can be attributed to Ce^{3+} ions occupying Ba^{2+} sites with an associated charge compensatory vacancy (Site II).[39]

As illustrated in Figs. 4 and 5, when terbium ions are codoped with cerium ions, the emission from Ce^{3+} ions decreases. On the other hand, codoping sodium along with cerium ions increases the emission due to Ce^{3+} ions. In comparison with curve III-b with IV-b in Figs. 4 and 5, it is also observed that the addition of Tb^{3+} ions to Ce^{3+}- and Na^+-codoped phosphors results in the quenching of Ce^{3+} emissions. In comparison with curve II-b with IV-b in Figs. 4 and 5, the addition of Na^+ ions to Ce^{3+}- and Tb^{3+}-codoped phosphors results in Ce^{3+} emission enhancement. These results are discussed in the next section.

Figure 6 illustrates the excitation spectra recorded for 543 nm emissions for (a) $Ba_{0.9}Tb_{0.1}BPO_5$, (b) $Ba_{0.89}Tb_{0.1}Ce_{0.01}BPO_5$, (c) $Ba_{0.885}Tb_{0.1}Ce_{0.01}Na_{0.005}BPO_5$, and (d) $Ba_{0.84}Tb_{0.1}Ce_{0.01}Na_{0.05}BPO_5$ phosphors. The excitation spectra are identical for all samples in the 350–400 nm range. The excitation peaks occurring at 275 and 315 nm in Ce^{3+}-codoped samples are intense, broad and similar to those of Ce^{3+} ions at two different sites observed in $Ba_{0.99}Ce_{0.01}BPO_5$, as discussed earlier. These observations

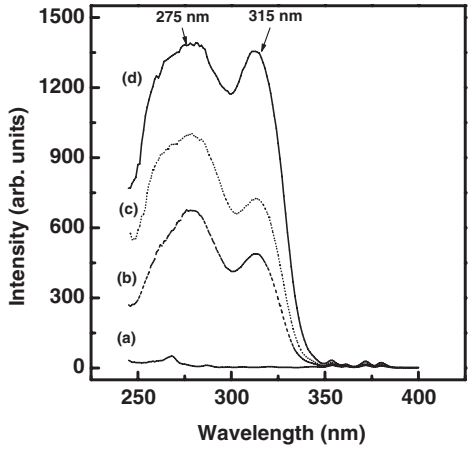

Fig. 6. Excitation spectra ($\lambda_{em} = 543$ nm) for phosphors prepared by heating at 900 °C for 4 h in reducing atmosphere: (a) $Ba_{0.9}Tb_{0.1}BPO_5$, (b) $Ba_{0.89}Tb_{0.1}Ce_{0.01}BPO_5$, (c) $Ba_{0.885}Tb_{0.1}Ce_{0.01}Na_{0.005}BPO_5$, and (d) $Ba_{0.84}Tb_{0.1}Ce_{0.01}Na_{0.05}BPO_5$.

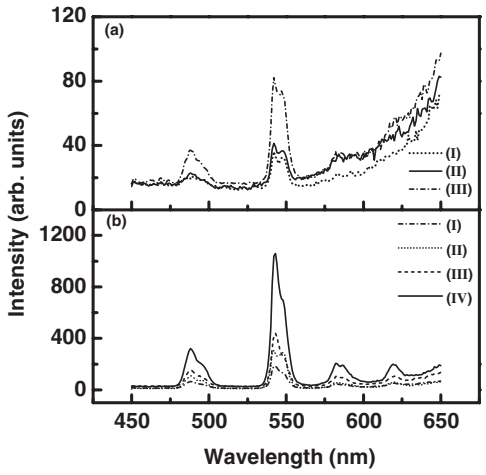

Fig. 7. Emission Spectra ($\lambda_{ex} = 254$ nm) for phosphors prepared by heating at 900 °C for 4 h in reducing atmosphere: (a) (I) $Ba_{0.9}Tb_{0.1}BPO_5$, (II) $Ba_{0.8995}Tb_{0.1}Ce_{0.0005}BPO_5$, and (III) $Ba_{0.899}Tb_{0.1}Ce_{0.001}BPO_5$ and (b) (I) $Ba_{0.895}Tb_{0.1}Ce_{0.005}BPO_5$, (II) $Ba_{0.89}Tb_{0.1}Ce_{0.01}BPO_5$, (III) $Ba_{0.885}$-$Tb_{0.1}Ce_{0.01}Na_{0.005}BPO_5$ and (IV) $Ba_{0.84}Tb_{0.1}Ce_{0.01}Na_{0.05}BPO_5$.

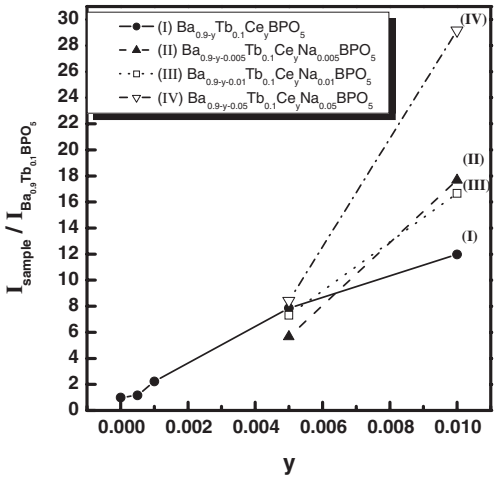

Fig. 8. Ratio of 254 nm excited emission intensity ($\lambda_{em} = 543$ nm) for phosphors prepared by heating at 900 °C for 4 h in reducing atmosphere to that for $Ba_{0.9}Tb_{0.1}BPO_5$ as a function of Ce^{3+} ion concentration: (I) $Ba_{0.9-y}Tb_{0.1}Ce_yBPO_5$, (II) $Ba_{0.9-y-0.005}Tb_{0.1}Ce_yBPO_5$, (III) $Ba_{0.9-y-0.01}$-$Tb_{0.1}Ce_yBPO_5$, and (IV) $Ba_{0.9-y-0.05}Tb_{0.1}Ce_yBPO_5$.

clearly suggest energy transfer from Ce^{3+} ions present at both sites to terbium ions in the phosphors. Similar to the Ce^{3+} ion substitution case at Ba^{2+} sites in $BaBPO_5$, Tb^{3+} ions are also expected to enter two distinct sites in the $BaBPO_5$ matrix owing to the incorporation of a charge compensatory vacancy. However, because of the shielding of $4f^8$ electrons from terbium ions from the anionic environment and low resolution of the spectrometer, $f \rightarrow f$ transitions do not reveal any notable difference in the $Ba_{0.9}Tb_{0.1}BPO_5$ excitation spectra. As shown in Figs. 4 and 5, the intensity of Ce^{3+} emissions (380 and 320 nm) is considerably reduced in $Ba_{0.84}Tb_{0.1}Ce_{0.01}Na_{0.05}BPO_5$ in comparison with that in $Ba_{0.94}Ce_{0.01}Na_{.05}BPO_5$. In $Ba_{0.89}$-$Tb_{0.1}Ce_{0.01}BPO_5$, a similar quenching of Ce^{3+} emissions is also observed on codoping Tb^{3+} ions along with Ce^{3+} ions. The results illustrated in Figs. 4–6 reveal that the quenching of Ce^{3+} emissions is associated with the transfer of energy to terbium ions in the codoped phosphors.

3.3 Effects of Na^+ ion codoping on luminescence properties

Figure 7 illustrates the emission spectra on 254 nm excitation observed for $Ba_{0.9-y-z}Tb_{0.1}Ce_yNa_zBPO_5$ phosphors. Nearly negligible emissions are observed for the $Ba_{0.9}Tb_{0.1}BPO_5$ phosphor [curve I in Fig. 7(b)]. As shown in curve I in Fig. 7(a) and curves II and III in Fig. 7(b), the emission from Tb^{3+} ions increases in $Ba_{0.9-y}Tb_{0.1}Ce_yBPO_5$ phosphors, whereas the amount of codoped Ce^{3+} ions varies in the 0.0005 to 0.01 range, when the Tb^{3+} concentration is maintained constant at 0.1. Curves II and III in Fig. 7(a) illustrate the emission spectra for $Ba_{0.885}Tb_{0.1}Ce_{0.01}$-$Na_{0.005}BPO_5$ and $Ba_{0.84}Tb_{0.1}Ce_{0.01}Na_{0.05}BPO_5$, respectively. The emission intensity markedly increases as a result of codoping sodium ions along with Ce^{3+} and Tb^{3+} ions in the phosphors. Among the spectra illustrated in Fig. 7(b) containing identical amounts of terbium ions, the most intense emission due to Tb^{3+} ions is observed in $Ba_{0.84}Tb_{0.1}Ce_{0.01}Na_{0.05}BPO_5$.

To understand the effects of codoping on the energy transfer and luminescence properties, the ratio of the emission intensity of the 543 nm peak on 254 nm excitation for $Ba_{0.9-y-z}Tb_{0.1}Ce_yNa_zBPO_5$ to that for $Ba_{0.9}Tb_{0.1}BPO_5$ is determined and illustrated in Fig. 8. As a result of codoping Ce^{3+} and Tb^{3+} ions, the emission intensity ratio ($I_{sample}/I_{Ba_{0.9}Tb_{0.1}BPO_5}$) increases with increasing Ce^{3+} ion concentration. The energy transfer occurs in the majority of cases through electric multipolar interactions. Depending on the type of multipolar interaction involved in the process, the energy transfer depends on the distance (R) between the two ions. The probability of energy transfer reveals an R^{-n} dependence, in which the n value depends on the type of multipolar interaction.[40] The total increase in energy transfer from Ce^{3+} ions to Tb^{3+} ions with increasing Ce^{3+} ion concentration in the phosphors is related to the decreasing distance between Ce^{3+} and Tb^{3+} ions.

The additional codoping of sodium ions along with Ce^{3+} and Tb^{3+} ions is observed to enhance the luminescence of Tb^{3+} ions. Similar enhancement in the luminescence of

Ce^{3+} ions is observed on codoping Na^+ ions (Figs. 4 and 5). The luminescence enhancement in these phosphors can occur due to several reasons: (a) energy transfer, (b) reduction in non-radiative transitions and (c) increased concentration of emitting ions. One of the requirements for the energy transfer to occur is the matching of energy levels for the two ions involved. In the case of Na^+ ions, because of their closed shell configuration, Na^+ ions cannot attain matching energy levels with Tb^{3+} and Ce^{3+} ions. The increase in the luminescence intensity of Ce^{3+} ions due to monovalent lithium ion codoping has been reported in lanthanum phosphate and is ascribed to the energy transfer from Ce^{4+} ions to Ce^{3+} ions facilitated by codoping.[41] Since most of the Ce^{4+} ions are reduced to Ce^{3+} ions during the reduction heat treatment, the absence of Ce^{4+} ions in the samples prepared in the reducing atmosphere rules out the possibility of energy transfer from Ce^{4+} ions to Ce^{3+} ions. Therefore, the increase in luminescence on codoping Na^+ ions with Ce^{3+} and Tb^{3+} ions in $BaBPO_5$ is most probably due to the reduction in non-radiative energy losses. Figure 9 shows the scanning electron micrographs of (a) $Ba_{0.89}Tb_{0.1}Ce_{0.01}BPO_5$ and (b) $Ba_{0.84}Tb_{0.1}Ce_{0.01}Na_{0.05}BPO_5$ heated at 900 °C for 4 h in reducing atmosphere. The effect of sodium ions is not considerably pronounced in changing the morphology and particle size of the samples; hence, we cannot solely attribute the enhanced efficiency to the sodium ions as a flux, as reported by Ding *et al.* for lithium ions,[20]

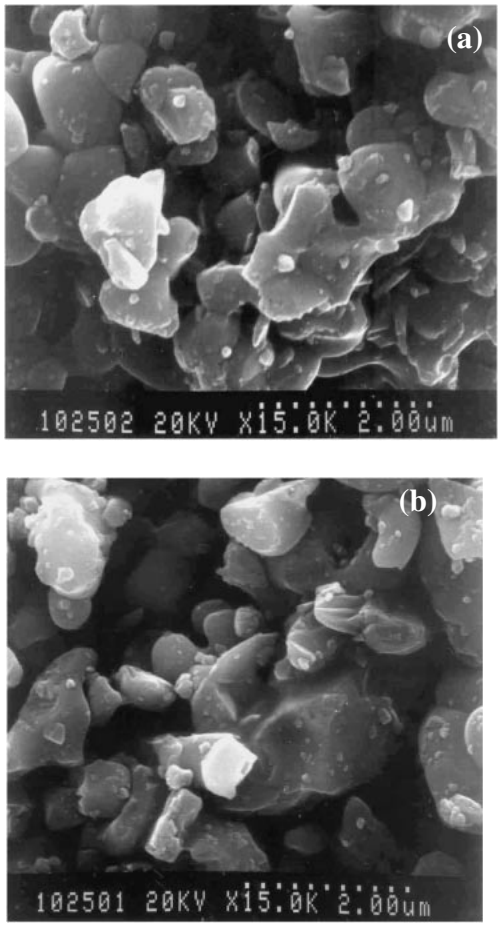

Fig. 9. Scanning electron micrographs of (a) $Ba_{0.89}Tb_{0.1}Ce_{0.01}BPO_5$ and (b) $Ba_{0.84}Tb_{0.1}Ce_{0.01}Na_{0.05}BPO_5$ heated at 900 °C for 4 h in reducing atmosphere.

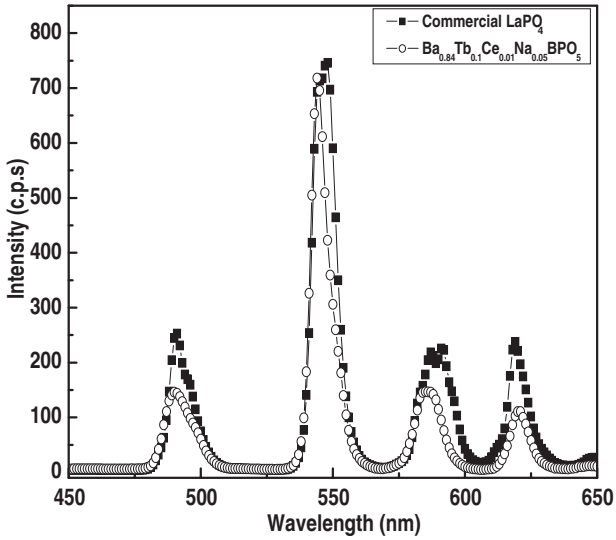

Fig. 10. Photoluminescence spectra of $Ba_{0.84}Tb_{0.1}Ce_{0.01}Na_{0.05}BPO_5$ and commercial $LaPO_4$ (excitation wavelength = 315 nm).

rather to the effect of reducing non-radiative transitions as mentioned above. We also compare the luminescence of our samples with that of the commercial $LaPO_4$ phosphor. Figure 10 shows the photoluminescence properties of $Ba_{0.84}Tb_{0.1}Ce_{0.01}Na_{0.05}BPO_5$ and commercial $LaPO_4$ (excitation wavelength = 315 nm). As can be clearly seen, the brightness of the samples synthesized in our group is comparable to that of the commercial samples. The relative quantum efficiency of the sample is measured as follows.[42]

$$QE_{\text{Sample}} = \frac{\text{Integrated emission of sample} \times QE_{\text{LaPO}_4}}{\text{Integrated emission of LaPO}_4}$$

QE is the quantum efficiency of the phosphor. The measured quantum efficiency of the sodium-doped sample is 0.56 in comparison with that of the commercial $LaPO_4$, which is 0.86 in the above-mentioned equation.

4. Conclusions

The luminescence properties of Tb^{3+} doped in a $BaBPO_5$ host were investigated in this study. The energy transfer on codoping Ce^{3+} and Tb^{3+} ions and the luminescence properties on codoping with Na^+ ions were also investigated. $BaBPO_5$:Tb^{3+} shows luminescence arising due to various $^5D_4 \rightarrow {}^7F_J$ ($J = 3$, 4, 5, and 6) transitions. The excitation in the 200–230 nm range in $BaBPO_5$:Tb^{3+} is ascribed to spin-allowed transitions. The relatively weak excitation band at 268 nm is related to spin-forbidden transitions. As a result of codoping Ce^{3+} ions, an additional intense excitation occurs in the 250–350 nm range due to energy transfer, as shown in the excitation spectra of Tb^{3+} ions. The energy transfer from Ce^{3+} ions to Tb^{3+} ions also results in quenching Ce^{3+} emissions in the phosphors. Codoping sodium ions in the phosphors is observed to enhance the luminescence, probably due to the reduction in non-radiative energy transfer. The phosphors containing Tb^{3+}, Ce^{3+}, and Na^+ ions in the $BaBPO_5$ host have potential for applications as green phosphors for tricolor lamps.

Acknowledgement

The authors would like to thank National Science Council,

Taiwan, R.O.C., for financially supporting this research under contract No. NSC 92-2214-E-002-036.

1) A. Levesseur, R. Olazcuaga, N. Kbala, N. Zahir, P. Haagenmuller and M. Couzi: Solid State Ionics **9** (1981) 205.
2) J. Koike, T. Kojima, R. Toyonaga, A. Kagami, T. Hase and S. Inaho: J. Electrochem. Soc. **126** (1979) 1008.
3) M. D. Faucher, R. Morlotti and O. K. Moune: J. Lumin. **96** (2002) 37.
4) Y. C. Kang, I. W. Lenggoro, K. Okuyama and S. B. Park: J. Electrochem. Soc. **146** (1999) 1227.
5) C. H. Lu, H. C. Hong and R. Jagannathan: J. Mater. Chem. **12** (2002) 2525.
6) C. H. Lu, W. T. Hsu, J. Dhanaraj and R. Jagannathan: J. Eur. Ceram. Soc. **24** (2004) 3723.
7) K. Ohno and T. Abe: J. Electrochem. Soc. **133** (1986) 638.
8) E. Nakazawa and S. Shionoya: J. Phys. Soc. Jpn. **28** (1970) 1260.
9) C. H. Lu, W. J. Hwang and S. V. Godbole: J. Mater. Res. **20** (2005) 464.
10) I. W. Lenggoro, B. Xia, H. Mizushima, K. Okuyama and N. Kijima: Mater. Lett. **50** (2001) 92.
11) R. P. Rao: J. Electrochem. Soc. **143** (1996) 189.
12) J. M. P. J. Verstegen, J. L. Sommerdijk and J. G. Verriet: J. Lumin. **6** (1973) 425.
13) J. L. Sommerdijk and J. M. P. J. Verstegen: J. Lumin. **9** (1974) 415.
14) S. Kamiya and H. Mizuno: *Phosphor Handbook* (CRC Press, Washington D.C., 1999) pp. 406, 416, 419, 426.
15) V. A. Pelova and L. S. Grigorov: J. Lumin. **72–74** (1997) 241.
16) F. S. Kao and T. M. Chen: J. Lumin. **96** (2001) 261.
17) C. H. Kam and S. Buddhudu: Mater. Lett. **54** (2002) 337.
18) H. X. Zhang, S. Buddhudu, C. H. Kam, Y. Zhou, Y. L. Lam, K. S. Wong, B. S. Ooi, S. L. Ng and W. W. Que: Mater. Chem. Phys. **68** (2001) 31.
19) Y. Kojima, S. Doi and T. Yasue: J. Ceram. Soc. Jpn. **110** (2002) 755.
20) S. J. Ding, D. W. Zhang, P. F. Wang and J. T. Wang: Mater. Chem. Phys. **68** (2001) 98.
21) D. D. Jia, J. Zhu and B. Q. Wu: J. Lumin. **93** (2001) 107.
22) T. Jüstel, D. U. Wiechert, C. Lau, D. Sendor and U. Kynast: Adv. Funct. Mater. **11** (2001) 105.
23) A. Karthikeyani and R. Jagannathan: J. Lumin. **86** (2000) 79.
24) L. C. Nehru, K. Marimuthu, M. Jayachandran, C. H. Lu and R. Jagannathan: J. Phys. D **34** (2001) 2599.
25) P. Dorenbos, L. Pierron, L. Dinca, C. W. E. van Eijk, A. Kahn-Harari and B. Viana: J. Phys.: Condens. Matter **15** (2003) 511.
26) H. B. Liang, Q. Su, Y. Tao, T. D. Hu, T. Liu and S. L. E. Shulin: J. Phys. Chem. Solids **63** (2002) 719.
27) Q. Zheng, N. Kilah and M. Riley: J. Lumin. **101** (2003) 167.
28) H. B. Liang, Q. Su, Y. Tao, T. D. Hu and T. Liu: J. Alloys Compd. **334** (2002) 293.
29) Q. Su, H. B. Liang, Y. Tao, T. D. Hu and T. Liu: J. Alloys Compd. **344** (2002) 132.
30) H. B. Liang, Q. G. Zeng, Y. Tao, S. Wang and Q. Su: Mater. Sci. Eng. B **98** (2003) 213.
31) X. T. Liu, G. X. Zhuang, F. S. Mo, Y. Z. Chen, Z. R. Ye and C. S. Shi: J. Rare Earth **18** (2000) 272.
32) H. Liang, Y. Tao, W. Chen, X. Ju, S. Wang and Q. Su: J. Phys. Chem. Solids **65** (2004) 1071.
33) ICDD file-19-0096.
34) G. H. Dieke: *Spectra and Energy Levels of Rare Earth Ions in Crystals* (Interscience Publishers, New York, 1968) p. 253.
35) J. L. Ryan and C. K. Jorgensen: J. Phys. Chem. **70** (1966) 2845.
36) M. J. J. Lammers and G. Blasse: J. Electrochem. Soc. **133** (1987) 2069.
37) J. W. M. Verwey, G. J. Dirksen and G. Blasse: J. Phys. Chem. Solids **53** (1992) 367.
38) V. P. Dotsenko, I. V. Berezovskaya, N. P. Efryushina, A. S. Voloshinovskii, P. Dorenbos and C. W. E. Van Eijk: J. Lumin. **93** (2001) 137.
39) C. H. Lu and S. V. Godbole: J. Mater. Res. **19** (2004) 2336.
40) G. Blasse and B. C. Grabmaier: *Luminescent Materials* (Springer-Verlag, New York, 1994) p. 92.
41) J. Lin, G. Yao, Y. Dong, B. Park and M. Su: J. Alloys Compd. **225** (1995) 124.
42) A. A. Bol and A. Meijerink: J. Phys. Chem. B **105** (2001) 10197.